ARCHIVES OF ELECTRICAL ENGINEERING VOL. 71(1), pp. 189–209 (2022)

DOI 10.24425/aee.2022.140205

Inter-harmonic parameter identification method based on transform with local maximum spectrum

LIN SUN[1] ✉, JING SONG[2], YAN JIN[1]

[1] *Wuchang University of Technology*
China

[2] *National University of Defense Technology*
China

e-mail: ✉*linqi0349486@163.com, {19404425/963531916}@qq.com*

(Received: 25.05.2021, revised: 21.10.2021)

Abstract: In order to improve the detection accuracy of harmonics/inter-harmonics in power systems, a new method of harmonic/inter-harmonic detection based on synchrosqueezed transform and the Hilbert operator based on local spectrum maximum is proposed. Firstly, the spectrum of inter-harmonic signals is obtained through short-time Fourier transform, and the local maximum value of the spectrum in the frequency direction is detected. Then, based on the maximum frequency of the spectrum, a new frequency redistribution operator and synchronous extraction operator are constructed. It combines the operators with ridge detection for the decomposition of harmonic/inter-harmonic signals, so as to obtain a series of intrinsic mode function (IMF) components. Finally, the instantaneous amplitude and frequency of the IMF components is obtained by using the Hilbert operator. Meanwhile, according to the instantaneous frequency mutation point in the spectrum, the starting and ending time of transient harmonics/inter-harmonics is located accurately. Based on a low signal-to-noise ratio (SNR), the wavelet packet method (WP), Hilbert Marginal Spectrum method (HMS), synchrosqueezing wavelet transform method (SST), the Hybrid SST method (HSST), enhanced empirical wavelet transform (EEWT) and the proposed method are used to identify the harmonic/inter-harmonic parameters, respectively. The experimental results show that the proposed LMSST method can effectively separate the steady-state and transient harmonic/inter-harmonic signals, and has higher detection accuracy and better noise robustness.

Key words: inter-harmonic, parameter identification, power system, synchrosqueezed transform, time-frequency analysis

1. Introduction

With the rapid development of power electronics and extensive application of non-linear power electronics, harmonic/inter-harmonic pollution in power systems is becoming more and more serious [1]. The impact of harmonics on power quality is also getting more and more attention. In the power system, there are not only integer harmonics whose frequency is integer multiple of power frequency, but also a large number of non-integer and fractional harmonics. These harmonics seriously affect the safe operation of the power system, and the control of them is necessary. The accurate detection of inter-harmonics is the premise of harmonic control. How to accurately obtain the instantaneous frequency and amplitude of inter-harmonics is the key for harmonic detection [2].

Power system harmonics are divided into steady-state harmonics and transient harmonics. The steady-state harmonics include steady-state integer harmonics and inter-harmonics, while the transient harmonics mainly include short-time harmonics and time-varying harmonics. For different applications, domestic and foreign scholars have conducted in-depth research and proposed different harmonic detection methods [3], mainly including instantaneous reactive power theory [4], the i_p-i_q algorithm [5], Fourier transform [6], wavelet transform [7], S-transform [8] and Hilbert-Huang transform (HHT) [9]. The instantaneous reactive power theory and the i_p-i_q algorithm have a small amount of calculation and good real-time performance. They are suitable for online harmonic detection, but a phase-locked loop is required to lock the grid synchronization angle. The instantaneous reactive power theory also requires a symmetrical and distortion-free signal. The Fourier transform method detects integer harmonics with high accuracy. But it cannot avoid frequency leakage and fence effects caused by non-synchronous sampling, and cannot analyse non-smooth signals, such as transient harmonics. Wavelet transform has a good time-frequency localisation effect, and can be used to locate the starting and ending moments of transient harmonics. However, the decomposition effect is highly dependent on the choice of wavelet basis and decomposition layers. S-transform uses a Gaussian window function for time-frequency transformation, which can achieve effective detection of transient signals, and its time-frequency resolution is still relatively fixed. The HHT method can perform adaptive decomposition of non-stationary and non-linear signals, and is capable of steady-state and transient harmonic analysis. However, over-envelope and under-envelope phenomena are prone to appear in decomposition. The decomposition of harmonic signals with similar frequencies may lead to modal mixing.

Reference [10] proposed a method of harmonic parameter identification based on Prony's method with energy analysis, but the problem that the energy of harmonics with small amplitude is similar to the energy of noise component is not considered, and the number of harmonics needs to be manually selected. Reference [11] proposed a harmonic detection algorithm for power grids, based on the combination of ensemble empirical mode decomposition-independent component analysis (EEMD-ICA) and singular value decomposition (SVD). This method requires no prior information of source signals and can separate harmonics from non-stationary signals. However, the EEMD-ICA-SVD method is sensitive to noise and requires a large amount of calculation. Reference [12] proposed a harmonic detection method based on visual merchandising (VMD), but it did not explain how to select an appropriate number of modal components. Reference [13] proposed a harmonic parameter detection method based on empirical wavelet

transform (EWT). The method first estimates the frequency component in the distorted signal, calculates the boundary value, and then filters according to the boundary value. Because this method does not need the prior information of the signal, the detection accuracy is better. In recent years, more harmonic detection algorithms have been proposed, such as the Kalman filter algorithm [14], instantaneous power theory (PQ) [15], sliding window Fourier analysis (SWFA) [16], the synchronous detection (SD) [17], the synchronous reference frame (SRF) theory or the d-q axis (DQ) [18], the synchronous detection with the Fourier (SDF) method [19], and the d-q axis with the Fourier (DQF) method [20].

Synchrosqueezed transform (SST) [21] is a new time-frequency analysis method proposed by Daubechies. SST squeezes the transformed time-frequency diagram in the frequency domain to obtain a time-frequency curve with high accuracy, so as to improve the frequency aliasing. However, SST still has some shortcomings [22]: firstly, when the frequencies of the signal components are relatively close, the lack of focus in the SST spectral domain will cause the signal spectrum to be blurred, which will seriously affect the analysis of instantaneous frequency. Secondly, when the signal is severely disturbed by noise, due to the lack of noise coefficient screening mechanism in the reconstruction of SST modal components, the extraction is greatly affected by noise, thus the analysis accuracy of modal component parameters is affected [23, 24].

In order to further improve the analysis capability of SST for complex signals, the local frequency maximum SST (LMSST) method is proposed. The method performs a short-time Fourier transform on the signal to obtain its spectrum; then, by detecting the local maxima of the spectrum in the frequency direction, a new frequency redistribution operator, namely a local maximum synchroextracting operator (LMSEO) is constructed, which has a higher time-frequency focusing capability and noise immunity than the traditional one. Combining the LMSEO operator with the ridge detection method can form an adaptive modal separation algorithm to achieve frequency division and cause effective separation of signal modal components. Due to the application of the local maximum synchroextracting operator, the LMSST overcomes the modal mixing of the traditional SST method for near-frequency signal analysis, and LMSST can successfully separate two time-varying harmonic components with similar frequencies. In addition, LMSST also has good noise robustness, because in the modal component extraction process, the coefficients are simultaneously screened according to the threshold and frequency. Simulations and actual data tests show that the LMSST method can sensitively detect the modal and time-varying features of the signal even in the data with low signal-to-noise ratios [25–27].

In view of the good band division, modal separation and noise immunity of LMSST for multi-component signals, this paper applies it to the parametric detection of inter-harmonic signals in power systems. Firstly, based on the STFT spectrum of inter-harmonic signals, a local maximum synchronous extraction operator is constructed. Then, the LMSST method is used to decompose the signal to obtain K state components, namely different harmonic and inter-harmonic modes. Finally, for the steady-state harmonic components, the Hilbert operator is used to demodulate the intrinsic mode function (IMF) component to obtain the instantaneous amplitude and frequency. For the transient harmonic component, the starting and ending time is located according to the mutation points in the spectrum. After that, the corresponding amplitude and frequency information in the duration is extracted through the Hilbert transform. The simulation results show that compared with the wavelet packet method (WP) [28], the Hilbert marginal spectrum method (HMS) [29], synchrosqueezing wavelet transform method (SST) [30], hybrid

SST method (HSST) [31] enhanced empirical wavelet transform (EEWT) and LMSST method has higher detection accuracy and better noise robustness, and can be applied to the parameter detection of steady-state and transient inter-harmonics.

2. Foundations of local frequency maximum synchrosqueezed transform

2.1. Short-time Fourier transform

A multi-component signal with amplitude modulation (AM) and frequency modulation (FM) is defined as$s(t)$ [24, 25].

$$s(t) = \sum_{k=1}^{K} A_k e^{i\varphi_k(t)}, \tag{1}$$

where A_k and the derivative $\varphi_k'(t)$ of $\varphi_k(t)$ are the instantaneous amplitude (IA) and instantaneous frequency (IF), respectively. IA and IF are two important instantaneous characteristics, which can be used to study the time-varying characteristics of multi-component signals. Assuming that real functions $s \in L^2(R)$ and $g \in L^2(R)$ are given as window functions, the short time Fourier transform (STFT) of the function s is defined as:

$$G(t,\omega) = \int_{-\infty}^{+\infty} g(u-t)s(u)e^{-i\omega(u-t)}\,\mathrm{d}u. \tag{2}$$

$G(t,\omega)$ is the spectrum of STFT. STFT can extend a one-dimensional time series signal to a two-dimensional time-frequency plane, which can effectively extract the instantaneous amplitude and instantaneous frequency of the signal. By integrating Eq. (2) in the frequency direction, Formula (3) can be obtained.

$$\int_{-\infty}^{+\infty} G(t,\omega)\,\mathrm{d}\omega = \int_{-\infty}^{+\infty}\int_{-\infty}^{+\infty} g(u-t)s(u)e^{-i\omega(u-t)}\,\mathrm{d}u\,\mathrm{d}\omega = 2\pi g(0)s(t). \tag{3}$$

Therefore, after STFT transform, the signal can be reconstructed as:

$$s(t) = (2\pi g(0))^{-1}\int_{-\infty}^{+\infty} G(t,\omega)\,\mathrm{d}\omega. \tag{4}$$

For multi-component signals, if the spectra of the components can be well separated in the time-frequency plane, the components can be reconstructed according to their instantaneous frequencies $\varphi_k'(t)$ and spectra $G(t,\omega)$.

$$s_k(t) = (2\pi g(0))^{-1}\int_{|\omega-\varphi_k'(t)|\le\varepsilon} G(t,\omega)\,\mathrm{d}\omega, \quad 1 \le k \le K. \tag{5}$$

2.2. Synchrosqueezed transform

For multi-component signals, according to the instantaneous amplitude $A_k(t)$ and instantaneous frequency $\varphi'_k(t)$ of each component signal, it can be expressed as [26]:

$$\mathrm{ITFA}(t,\omega) = \sum_{k=1}^{n} A_k(t) e^{i\varphi_k(t)} \delta(\omega - \varphi'_k(t)). \tag{6}$$

In the time-frequency (TF) analysis of signals, we assumed that the TF spectrum of each component is clear and separated from each other. However, due to spectrum leakage and mode aliasing, the spectrum of STFT is seriously blurred and the instantaneous frequency resolution is low. In order to observe the characteristics of time-varying TF more accurately, Daubechies *et al.* [21] proposed synchrosqueezed transform (SST). SST is defined as:

$$\mathrm{SST}(t,\eta) = \int_{-\infty}^{+\infty} G(t,\omega)\delta(\eta - \omega_0(t,\omega))\,\mathrm{d}\omega, \tag{7}$$

where

$$\omega_0(t,\omega) = \frac{\partial_t G(t,\omega)}{iG(t,\omega)}. \tag{8}$$

Substituting Eq. (2) into Eq. (8), we get the following equation:

$$\omega_0(t,\omega) = \omega + i\frac{G^g(t,\omega)}{G(t,\omega)} = \omega - \mathrm{Im}\left(\frac{G^g(t,\omega)}{G(t,\omega)}\right). \tag{9}$$

SST only considers the redistribution of frequency directions, e.g. $(t,\omega) \to (t,\omega(t,\omega))$. It turns out that for a purely harmonic signal $\varphi(t) = a + bt$. The result of SST transform is equivalent to its ideal instantaneous frequency according to iterative transformation factor analysis (ITFA), and SST can also reconstruct the components of a multi-component signal. The reconstructed equation for the component signal can be obtained through Eq. (4), the SST transform coefficients $\mathrm{SST}(t,\omega)$ and the instantaneous frequency $\varphi'_k(t)$.

$$s_k(t) = (2\pi g(0))^{-1} \int_{|\omega-\varphi'_k(t)|\le\varepsilon} \mathrm{SST}(t,\omega)\,\mathrm{d}\omega, \tag{10}$$

where ε denotes the reconstructed bandwidth of SST.

2.3. Local frequency maximum synchrosqueezed transform

Although the time-frequency analysis capability of SST is improved to a greater extent than STFT, when the frequency of component signal is relatively close or seriously polluted by noise, there is still a certain degree of spectrum chaos. This leads to different degrees of errors in signal instantaneous frequency calculation and component reconstruction. In order to solve the above problems and further improve the parameter detection accuracy of inter-harmonic signals in the power systems, this paper proposes a new SST model based on the local maximum

synchroextracting operator (LMSEO) – the local frequency maximum spectrum synchrosqueeze transform (LMSST) [23]. Set the spectrum of multi-component signal as:

$$|G(t,\omega)| = \sum_{k=1}^{n} A_k(t)\hat{g}\left(\omega - \varphi_k'(t)\right). \tag{11}$$

Based on Eq. (11), a new frequency redistribution operator is defined in this paper.

$$\omega_m(t,\omega)| = \begin{cases} \underset{\omega}{\operatorname{argmax}} |G(t,\omega)|, \omega \in [\omega-\Delta, \omega+\Delta], & \text{if } \|G(t,\omega)\| \neq 0 \\ 0, & \text{if } |G(t,\omega| = 0 \end{cases}. \tag{12}$$

Assuming that the frequency distance between any two modes in the multi-component signal satisfies $\varphi_{k+1}'(t) - \varphi_k'(t) > 4\Delta k \in 1, 2, \cdots n-1\}$, and considering that the Fourier transform of the window function reaches the maximum value at zero, namely $\hat{g}(\omega) \leq \hat{g}(0)$, the results are as follows:

$$\omega_m(t,\omega)| = \begin{cases} \varphi_k'(t), & \text{if } \omega \in [\varphi_k'(t)-\Delta, \varphi_k'(t)+\Delta] \\ 0, & \text{otherwise} \end{cases}. \tag{13}$$

From the above analysis, it is clear that the only way to improve the reconstruction capability of multi-component signal modal components is to redistribute the TF coefficients in the frequency direction. Therefore, the local frequency maximum synchrosqueezed transform (LMSST) is defined as:

$$\mathrm{LMSST}(t,\eta) = \int_{-\infty}^{+\infty} G(t,\omega)\delta(\eta - \omega_m(t,\omega))\,\mathrm{d}\omega. \tag{14}$$

To demonstrate the signal reconstruction capability of LMSST, the following expressions are constructed:

$$\begin{aligned} \int_{-\infty}^{+\infty} \mathrm{LMSST}(t,\eta)\,\mathrm{d}\eta &= \int_{-\infty}^{+\infty}\int_{-\infty}^{+\infty} G(t,\omega)\delta(\eta - \omega_m(t,\omega))\,\mathrm{d}\omega\,\mathrm{d}\eta = \\ &= \int_{-\infty}^{+\infty} G(t,\omega)\int_{-\infty}^{+\infty}\delta(\eta - \omega_m(t,\omega))\,\mathrm{d}\eta\,\mathrm{d}\omega = \\ &= \int_{-\infty}^{+\infty} G(t,\omega)\,\mathrm{d}\omega = (2\pi g(0))s(t). \end{aligned} \tag{15}$$

Thus, after the LMSST, the signal can be reconstructed entirely.

$$s(t) = (2\pi g(0))^{-1}\int_{-\infty}^{+\infty} \mathrm{LMSST}(t,\omega)\,\mathrm{d}\omega. \tag{16}$$

From Eq. (16), the reconstruction formula for each modal component can be written as follows:

$$s_k(t) = (2\pi g(0))^{-1}\mathrm{LMSST}(t,\varphi_k'(t)). \tag{17}$$

3. Inter-harmonic detection based on local frequency maximum synchrosqueezed transform

3.1. Inter-harmonic signal instantaneous frequency trajectory detection

The detection of inter-harmonic parameters using the local frequency maximum synchrosqueezed transform (LMSST) algorithm relies, to a large extent, on the estimation of the instantaneous frequency ridges. The difficulty lies in how to accurately detect the instantaneous frequency (IF) trajectory of the inter-harmonics [32, 33]. In this paper, the method in [27] is used to detect the inter-harmonic instantaneous frequency trajectory in the spectrum, and the instantaneous frequency trajectory detection equation is TFR IF.

$$E(\mathrm{IF}_k(t)) = \int_{-\infty}^{+\infty} |\mathrm{TFR}(t, \mathrm{IF}_k(t))|^2 \,\mathrm{d}t - \int_{-\infty}^{+\infty} \left(\lambda \cdot \mathrm{IF}_k'(t) + \beta \cdot \mathrm{IF}_k'(t)^2\right) \mathrm{d}t, \tag{18}$$

where $(t, \mathrm{IF}_k(t))$ is the IF trajectory of the K-th mode estimate of the inter-harmonic signal in the TF plane. λ and β are two regularisation parameters. In the instantaneous frequency trajectory detection of an inter-harmonic signal, the transient frequency ridge with the largest energy mode component is first detected according to Eq. (18). The specific steps are as follows: firstly, the whole TF plane of the inter-harmonic signal is segmented according to the energy partition, and the starting point of the instantaneous frequency trajectory is found; secondly, the forward and backward search schemes are implemented to search the IF trajectory; finally, the best IF trajectory is selected from these tracks according to the local frequency energy maximum criterion. After TF is solved, the trajectories are estimated to be zero. The trajectories of all modes in the inter-harmonic signals can be estimated by multiple iterations.

3.2. Inter-harmonic mode component extraction based on synchroextracting operator

The actual inter-harmonic signals of the power system usually contain a lot of noise, which is submerged by noise and seriously affects the detection accuracy of inter-harmonic parameters. In order to eliminate the influence of noise, a local maximum synchroextracting operator (LMSEO) is introduced into LMSST to extract the inter harmonic components. The one-dimensional IF function for the first component of a multi-component inter-harmonic signal is expressed as:

$$\mathrm{IF}_k(t) = \varphi_k'(t). \tag{19}$$

The Dirac function can be extended to a two-dimensional TF plane:

$$\mathrm{IF}_k(t, \omega) = \delta\left(\omega - \varphi_k'(t)\right). \tag{20}$$

Based on Eq. (20), a local maximum synchroextracting operator (LMSEO) is constructed:

$$\mathrm{LMSEO}(t, \omega) = \delta(\omega - \omega_m(t, \omega)). \tag{21}$$

It can be seen from Eq. (13) that $\omega_m(t, \omega)$ is the superposition of IF at each mode. Substituting it into Eq. (20), we can obtain as follows:

$$\delta(\omega - \omega_m(t, \omega)) = \begin{cases} 1, & \text{if } \omega = \varphi_k'(t) \\ 0, & \text{otherwise} \end{cases}. \tag{22}$$

From Eq. (22), it can be seen that the LMSEO is very close to the instantaneous frequency of the inter-harmonic signal and can be used to represent the time-varying characteristics of the instantaneous frequency. Taking into account the calculation errors in practical applications, an error factor is introduced and the LMSEO is redefined as:

$$\mathrm{LMSEO}(t,\omega) = \begin{cases} 1, & |\omega - \omega_m(t,\omega)| < \varepsilon \\ 0, & \text{otherwise} \end{cases}. \tag{23}$$

In order to ensure that the IF trajectory of each extracted modal component does not exceed the TF plane, the following constraints are added.

$$0 < \varphi_k'(t) < (SF)/2,\ \forall, t \in R \ \text{ and } \ \forall\, k \in 1, 2, \cdots n. \tag{24}$$

In Eq. (24), SF denotes the sampling frequency.

Given the inter-harmonic signal $s(t), t = t_0 \cdots t_{N-1}$ the instantaneous frequency trajectory detection of the component signal is first performed by Eq. (18). On the basis of the IF trajectory detection, the LMSST and LMSEO joint methods are used to decompose and extract the components of inter-harmonic signals. The termination condition for component extraction is shown in Eq. (25).

$$\sum_{n=0}^{N-1} \mathrm{FMSEO}(t_n, \mathrm{IF}_k(t_n)) > \rho N, \tag{25}$$

where ρ is the constant threshold, and the value is $\rho = 0.8$.

3.3. Calculation of inter-harmonic parameters

The signals with inter-harmonics in the power system can be expressed as follows:

$$f(t) = \sum_{k=1}^{K} A_k \cos(2\pi\omega_k t + \phi_k), \tag{26}$$

where: A_k is the amplitude; ω_k is the frequency, and ϕ_k is the initial phase. Since LMSST extracts the intrinsic mode function (IMF) components corresponding to different harmonic components, the process of detecting IMF components is actually the process of detecting harmonics.

The IMF function model can be expressed as:

$$f_k(t) = A_k \cos(2\pi\omega_k t + \phi_k). \tag{27}$$

In order to obtain the amplitude, frequency and phase of the k-th harmonic component, it is sufficient to detect A_k, ω_k and ϕ_k, and the Hilbert transform of the k-th component $f_k(t)$ extracted by SST:

$$y(t) = \frac{1}{\pi} \int_{-\infty}^{+\infty} \frac{f_k(t)}{t-\tau}\,\mathrm{d}t. \tag{28}$$

The inverse Hilbert transform is obtained by exchanging y and f_k in Eq. (9), thus we obtain the analytic signal.

$$z(t) = f_k(t) + iy(t) = A(t)e^{i\theta(t)}, \tag{29}$$

where

$$A(t) = \sqrt{f_k^2(t) + y^2(t)}, \qquad \theta(t) = \arctan\left[\frac{y(t)}{f_k(t)}\right]. \tag{30}$$

Then the amplitude A_0 and the frequency ω_d of the harmonic signal are calculated as:

$$A_0 = A(t), \qquad \omega_d = \frac{1}{2\pi}\frac{\mathrm{d}\theta}{\mathrm{d}t}. \tag{31}$$

Since the amplitude A_0 and frequency ω_d are calculated by Eq. (30) and Eq. (31), the values of A_0 and ω_d will slightly change, and the final detection values of A_0 and ω_d can be calculated by least squares fitting.

It can be seen from the above that the LMSST algorithm can extract the inter-harmonics through the following steps, and the flow chart of LMSST is shown in Fig. 1.

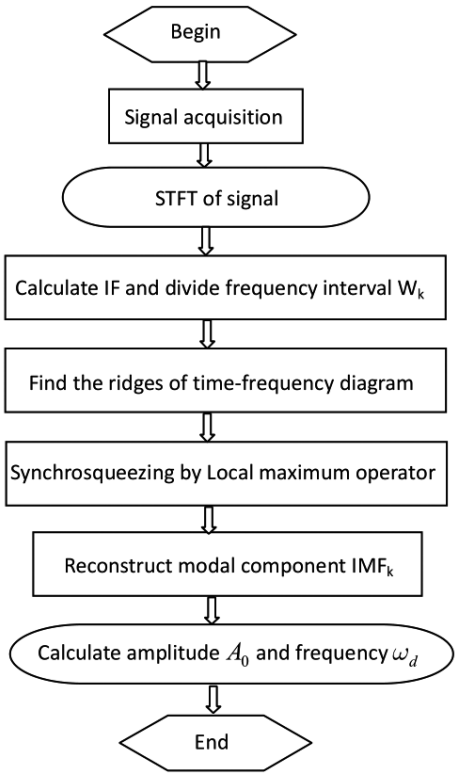

Fig. 1. Flow chart of LMSST method

Step 1: The continuous wavelet transform $W_f(a,b)$ on the power signal f containing inter-harmonics is carried out. The discretization of $W_f(a,b)$ gives $\widetilde{W}_f(a_j,t_m)$, and the discretization of the instantaneous frequency obtained from Eq. (2) gives $\widetilde{\omega}_f(a_j,t_m)$.

Step 2: Divide frequency intervals. Assuming that the power signal $f(t)$ containing inter-harmonics has length $n = 2^{L+1}$ and sampling time interval Δt, take $n_v = 32$, and let $n_a = Ln_v$,

$$\Delta\omega = \frac{1}{n_a - 1}\log_2\left(\frac{n}{2}\right), \qquad \omega_0 = \frac{1}{n\Delta t}.$$

Specify $\omega_l = 2^{l\Delta\omega}\omega_0$ and $l = 0, 1, \cdots, n_a - 1$, then according to the Nyquist sampling theorem, the frequency range of the power system harmonic signals can be divided into different frequency intervals

$$W_l = \left[\frac{\omega_{l-1} + \omega_l}{2}, \frac{\omega_l + \omega_{l+1}}{2}\right].$$

Step 3: Discrete synchronous extrusion $\widetilde{T}_f(\omega_l, b)$ in the time-frequency plane: the synchronous squeezing wavelet transform of signals at the center frequency ω_l is as follows:

$$\widetilde{T}_f(\omega_l, b) = \sum_{\substack{0\le j\le n_a-1,\\ j:\ |\widetilde{\omega}(a_j,t_m)|\in W_l}} \widetilde{W}_f\left(a_j t_m\right)\frac{\log 2}{n_v}a_j^{-\frac{1}{2}},$$

where $t_m = m\Delta t$.

Step 4: Extraction of each harmonic inter-harmonic and fundamental component signal. The k-th component (fundamental, harmonic or inter-harmonic) can be reconstructed from Eq. (5).

$$f_k(t_m) = \frac{2}{R_\psi}\mathrm{Re}\left(\sum_{l\in L_k(t_m)}\widetilde{T}_f(\omega_l, t_m)\right),$$

where, $L_k(t_m)$ is the subscript set of ω_l around the narrow band of the curve f_k.

Step 5: The IMF component $f_k(t)$ of LMSST is transformed by Hilbert transform. Then the amplitude A_0 and frequency ω_d are calculated by Eq. (30) and Eq. (31). The final detection values of A_0 and ω_d are obtained by least square fitting.

4. Experimental and numerical validation

4.1. Steady-state harmonic analysis

Assume that the power signal containing steady-state harmonics is $x(t)$.

$$x(t) = 15\cos(100\pi t) + 3.5\cos(150\pi t) + 30\cos(250\pi t) + 55\cos(300\pi t) + +10\cos(500\pi t) + n(t).$$

The signal $x(t)$ contains fundamental, 3rd and 5th harmonics, and 1.5 and 2.5 inter-harmonics, and a Gaussian white noise with $n(t)$ of 30 dB is added to the signal $x(t)$ to form the original signal. The sampling frequency of the signal is 5120 Hz, and the sampling time is 1 s. Figure 2 shows the time domain waveform of the original signal.

This signal spectrum is shown in Fig. 3.

In order to compare the detection accuracy of the proposed method for harmonic/interharmonic parameters, the Wavelet Packet method (WP) [28], Hilbert Marginal Spectrum method

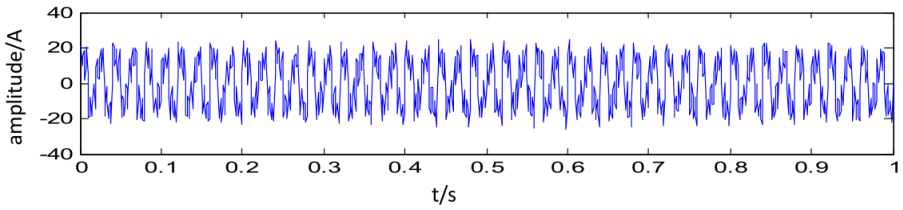

Fig. 2. Time domain waveform of original signal

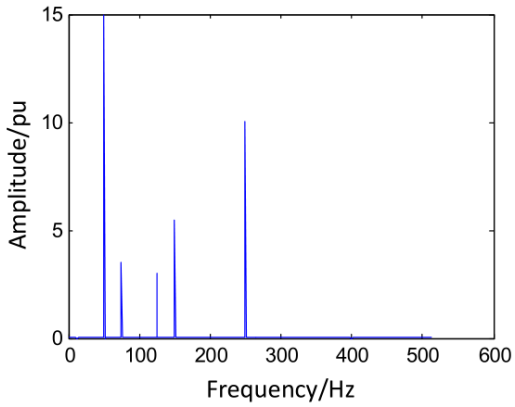

Fig. 3. Spectrum of steady state inter-harmonic signal

(HMS) [29], Synchrosqueezing Transform method (SST) [30], Hybrid Synchrosqueezing Transform method (HSST) [31], Enhanced Empirical Wavelet Transform (EEWT) and the proposed LMSST method are used to detect the parameters of analog harmonic signals. Firstly, the original signal containing noise is decomposed by the WP, EMD, SST, HSST, EEWT and LMSST, respectively, and the signal is not de-noised in decomposition. The standard deviation of the added Gaussian white noise amplitude is 0.2, the set averages is set to 200, and the modal components of SST and LMSST is $K = 5$. The decomposition results are shown in Fig. 4(a) and Fig. 4(b) (only the graph of [0 s, 0.25 s] is drawn for clarity).

Figure 4(a) shows the SST decomposition results of the original signal full of noise, where IMF1 is the fundamental component, IMF5 is the 5th harmonic component, and IMF2-IMF4 is the remaining harmonic components. IMF2-IMF5 show that modal aliasing occurs. Due to the effect of noise and spectral mixing, SST cannot accurately decompose each harmonic/inter-harmonic. Figure 4(b) shows the components obtained from the decomposition of LMSST. IMF1-IMF5 are arranged in the order of fundamental wave, 1.5 and 2.5 inter-harmonics, 3rd and 5th harmonics. From the waveform, it can be seen that each component is basically a single frequency harmonic and no modal aliasing occurs.

In order to visualise the time-varying characteristics of the amplitude and frequency of LMSST components, the Hilbert operator is used to demodulate the individual modal components in Fig. 4(b). The instantaneous amplitude and frequency of the modal components are shown in

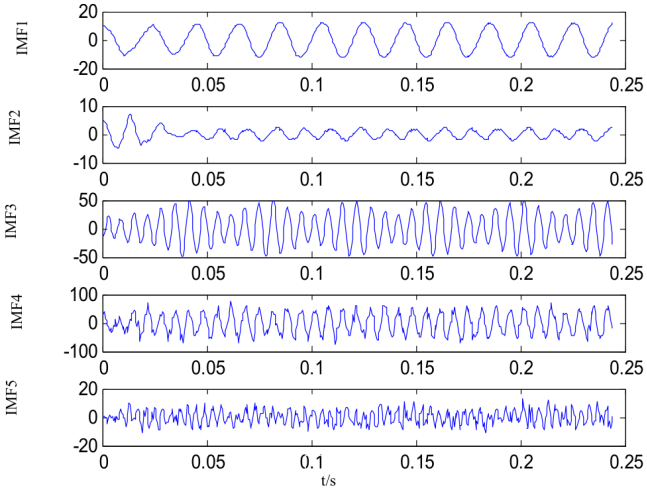

(a) Decomposition results of SST

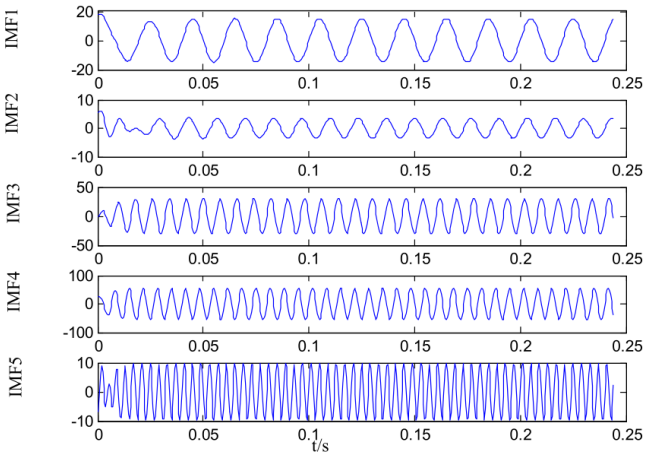

(b) Comparison of main harmonic components of no-load B-EMF of part of the skew structure

Fig. 4. Decomposition results of steady state harmonics

Fig. 5(a) and Fig. 5(b). From Fig. 5(a) and Fig. 5(b), the instantaneous amplitudes and frequencies of the modal components are basically a straight line, except for the deviations at the endpoints. This indicates that the detected values are close to the theoretical values. In order to compare the parameter detection results of SST and LMSST, the component of Fig. 4(a) obtained after the decomposition of SST is also subjected to Hilbert operator demodulation analysis.

In order to compare the parameter detection results of the six methods, the decomposition results of the WP, EMD, SST, HSST and EEWT are demodulated and analysed by the Hilbert

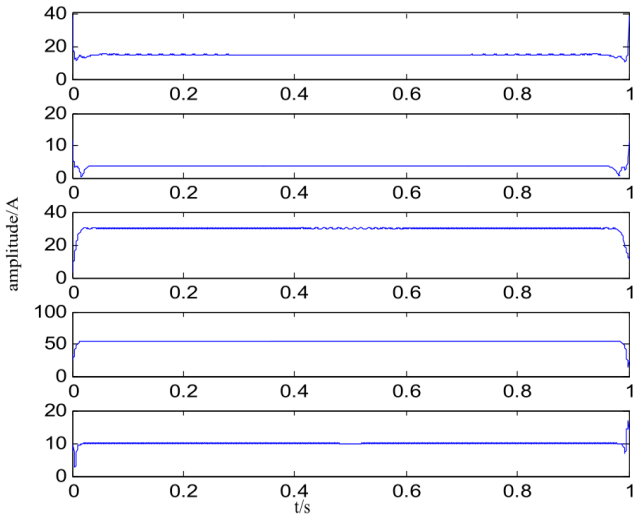

(a) Identification of instantaneous amplitude by LMSST

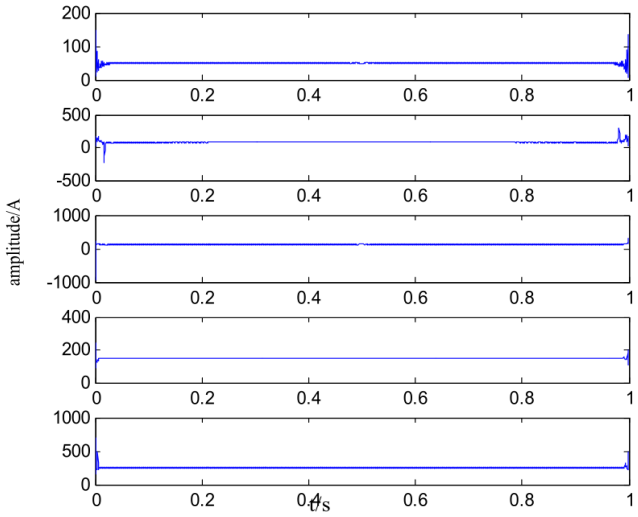

(b) Identification of instantaneous frequency by LMSST

Fig. 5. Instantaneous amplitude and frequency of steady harmonic

operator. Then, for the waveform after demodulation analysis, the average value of other parts except the endpoint is obtained. It is used as the detection value of steady-state harmonic component parameters, and the results are shown in Table 1.

It can be seen from Table 1 that, the average errors of amplitude and frequency detection by the WP method are 1.972% and 1.082%, respectively; by the HMS method are 1.599% and

Table 1. Identification results of steady harmonic component parameters

Method	**Actual**	**Modal components**									
		IMF1		**IMF2**		**IMF3**		**IMF4**		**IMF5**	
		ampl	freq	ampl	freq	ampl	freq	ampl	freq	ampl	freq
		15.0	50.00	3.50	75.00	30.0	125.0	55.0	150.0	10.0	250.0
WP	Estimated	14.586	50.822	3.457	74.081	30.497	125.929	54.183	151.268	10.273	252.379
	Error	2.760%	1.644%	1.228%	1.225%	1.656%	0.743%	1.485%	0.845%	2.730%	0.952%
HMS	Estimated	14.624	50.729	3.452	74.113	30.340	124.095	54.274	151.192	9.834	252.184
	Error	2.511%	1.458%	1.371%	1.182%	1.133%	0.724%	1.320%	0.795%	1.660%	0.874%
SST	Estimated	14.829	50.646	3.469	74.209	30.283	124.163	54.297	150.912	10.088	248.033
	Error	1.135%	1.092%	0.877%	1.054%	0.944%	0.669%	1.095%	0.608%	0.889%	0.787%
HSST	Estimated	14.865	49.641	3.483	74.502	29.711	124.572	54.594	150.617	9.914	249.281
	Error	0.900%	0.718%	0.485%	0.664%	0.963%	0.342%	0.738%	0.411%	0.860%	0.288%
EEWT	Estimated	14.877	50.320	3.488	75.427	30.231	124.629	54.616	149.611	10.034	249.471
	Error	0.820%	0.640%	0.342%	0.569%	0.770%	0.297%	0.698%	0.259%	0.340%	0.212%
LMSST	Estimated	14.889	49.698	3.509	74.597	29.797	125.301	54.659	150.302	9.979	249.599
	Error	0.737%	0.602%	0.260%	0.536%	0.677%	0.241%	0.621%	0.201%	0.203%	0.160%

1.007%, respectively; by the SST method are 0.988% and 0.842%, respectively; by the HSST method are 0.789% and 0.484%, respectively; by the EEWT method are 0.594% and 0.396%, respectively and that by the LMSST method are 0.499% and 0.348%, respectively.

According to the test results, the detection accuracy of the LMSST method is significantly higher than that of WP, HMS, SST and HSST methods. The EEWT method also has high detection accuracy, but compared with the EEWT method, the detection accuracy of the LMSST method proposed in this paper is still improved to a certain extent. This is because the adaptive mode decomposition algorithm formed by the combination of the ridge detection method and the synchronous extraction operator of the LMSST algorithm can effectively decompose the inter-harmonic signal into multiple single components, and reduce the influence of noise on the signal decomposition. From Fig. 5(b) and Table 1, it can be seen that the LMSST method still has high detection accuracy when detecting harmonic/inter-harmonic signals with noise. It indicates that LMSST also has good robustness to noise.

4.2. Transient harmonic analysis

Assuming that the power signal with transient harmonics is $x(t)$.

$$\begin{aligned} x_1(t) &= 15\cos(100\pi t), & 0 \le t \le 0.4, \\ x_2(t) &= 3.5\cos(350\pi t), & 0.05 \le t \le 0.3, \\ x(t) &= x_1(t) + x_2(t). \end{aligned}$$

The signal consists of the fundamental and 3.5th inter-harmonic. The 3.5th inter-harmonic is superimposed into the signal at 0.05 s and stops superimposing at 0.3 s. The fundamental frequency is 50 Hz, the sampling frequency is 5120 Hz and the sampling time is 0.4 s. Fig. 6 shows the time domain waveform of the transient harmonic signal.

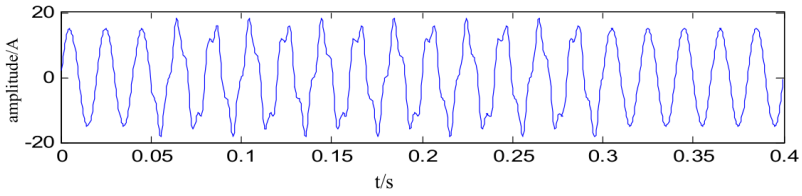

Fig. 6. Time domain waveform of transient harmonic signal

Set the modal components $K = 2$. The WP, HMS, SST, Hybrid-SST, EEWT and LMSST are used to decompose transient harmonic signals respectively. Due to space limitation, only decomposition results of SST and LMSST are presented in this paper, as shown in Fig. 7(a) and Fig. 7(b). From Fig. 7, it can be seen that although the method can decompose the transient

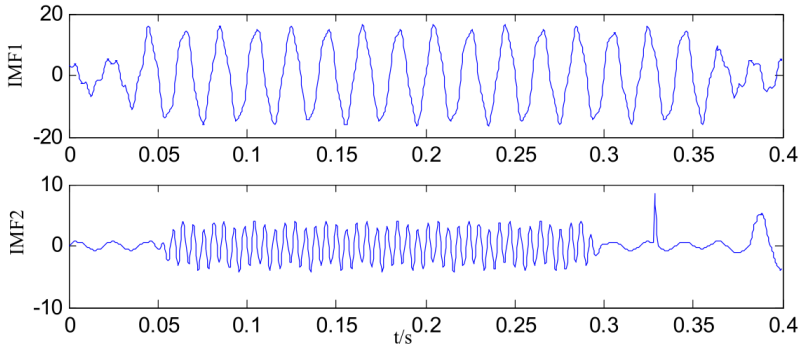

(a) Decomposition results of SST

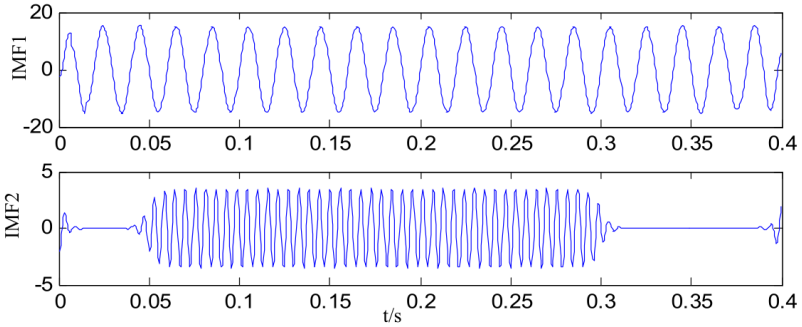

(b) Decomposition results of LMSST

Fig. 7. Decomposition results of state inter-harmonics

harmonics from the signal, there is still some modal mixing in these two components. IMF1 and IMF2 components obtained from the decomposition in Fig. 7(b) correspond to the fundamental wave and the short-time inter-harmonic 3.5, respectively. These two components are basically sinusoidal waves with clear decomposition levels, indicating that the LMSST algorithm has strong decomposition capability.

The decomposition results of the six methods are analyzed by Hilbert operator demodulation, and the instantaneous amplitude and frequency waveforms of the components are obtained. Due to space limitation, only the demodulation analysis results of LMSST decomposition components are shown in Fig. 8(a)–Fig. 8(d). According to Fig. 8(d), it can be seen that a mutation point

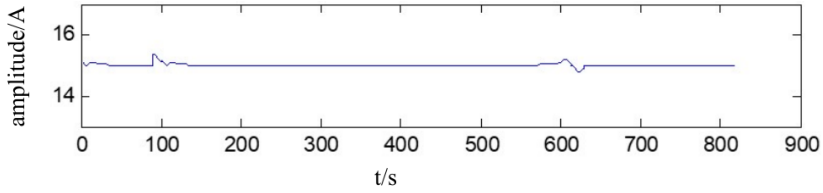

(a) Instantaneous amplitude of IMF1

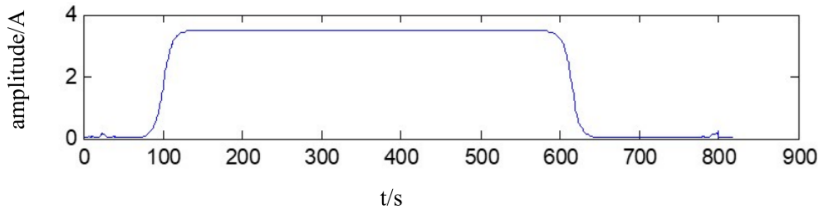

(b) Instantaneous frequency of IMF1

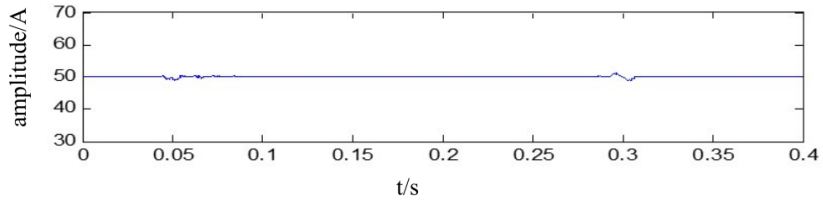

(c) Instantaneous amplitude of IMF2

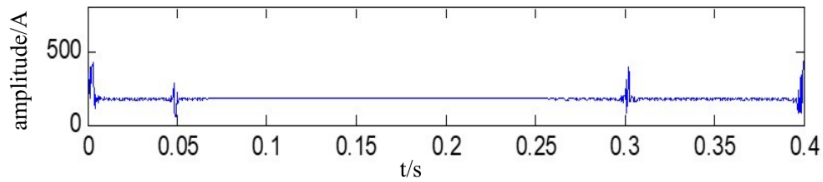

(d) Instantaneous frequency of IMF2

Fig. 8. Analysis results of transient inter harmonic signal

appears at the starting and ending of the transient harmonics. The starting time of the 1.5th inter-harmonic obtained from LMSST decomposition is 0.0503 s and the ending time is 0.3017 s. Similarly, the starting and ending time of the WP method is 0.0457 s and 0.3211 s, respectively; that of the HMS method is 0.0461 s and 0.3227 s, respectively; that of the SST method is 0.0467 s and 0.3192 s, respectively; that of the HSST method is 0.0492 s and 0.3068 s and that of the EEWT method is 0.0495 s and 0.3028 s, respectively. The comparison between the detection results of the six methods and the theoretical values is shown in Table 2.

Table 2. Detection results of transient harmonic starting and ending time

Method	**Starting time/s**			**Ending time/s**		
	Actual	**Detected**	**Error/%**	**Actual**	**Detected**	**Error/%**
WP	0.0500	0.0457	8.600	0.3000	0.3211	7.033
HMS	0.0500	0.0461	7.800	0.3000	0.3227	7.566
SST	0.0500	0.0467	6.600	0.3000	0.3192	6.400
HSST	0.0500	0.0492	1.600	0.3000	0.3068	2.266
EEWT	0.0500	0.0495	1.000	0.3000	0.3028	0.933
LMSST	0.0500	0.0503	0.600	0.3000	0.3017	0.567

According to Table 2, the accuracy of the LMSST positioning start and end time is significantly higher than that of the WP, HMS, SST and HSST. Although the accuracy of the EEWT positioning start and end time is relatively high, it is still lower than that of the LMSST method. The reason is that the LMSST algorithm uses the local maximum synchroextracting operator (LMSEO) to continuously update each mode and its central frequency, so that the transient harmonics in the signal can be accurately and thoroughly decomposed. This makes the sudden change point of the starting and ending moments of instantaneous frequency very obvious, so as to accurately locate the starting and ending moments. The average value of the smoothed phase from the starting to the ending of the moment in Fig. 8(c) and Fig. 8(d) is used as the detection value of the instantaneous amplitude and frequency of the 3.5th inter-harmonic component. The average of the waveforms in Fig. 8(a) and Fig. 8(b) is taken as the detected value of the instantaneous amplitude and frequency of the fundamental waveform. The parameters detection results of each component of transient harmonics are shown in Table 3.

According to the detection results in Table 3, the average error of amplitude and frequency detection by the WP method is 1.819% and 1.463%, respectively; by the HMS method are 1.888% and 1.509%, respectively; by the SST method are 1.404 and 1.215, respectively; by the HSST method are 0.821% and 0.480%, respectively; by the EEWT method are 0.651% and 0.272%, respectively and by the proposed LMSST method are 0.537% and 0.186%, respectively. It can be seen that compared with the other four methods, the proposed method has the lowest error in detecting the amplitude and frequency of inter-harmonic, and the detection effect is better.

Table 3. Detection results of transient harmonic component parameters

Method	Actual	Modal components			
		IMF1		IMF2	
		Ampl	Freq	Ampl	Freq
		15.000	50.000	3.50	175.00
WP	Estimated	14.8247	49.1362	3.4188	177.0974
	Error	1.318%	1.727%	2.320%	1.198%
HMS	Estimated	14.7622	49.0407	3.4233	176.9255
	Error	1.585%	1.918%	2.191%	1.100%
SST	Estimated	14.8537	49.2745	3.4358	176.7136
	Error	0.975%	1.451%	1.834%	0.979%
HSST	estimated	14.9032	49.6275	3.4651	174.6216
	Error	0.645%	0.745%	0.997%	0.216%
EWWT	Estimated	15.0817	50.1872	3.5265	175.2971
	Error	0.544%	0.374%	0.757%	0.169%
LMSST	Estimated	15.0721	49.8768	3.4792	174.7818
	Error	0.481%	0.247%	0.594%	0.125%

4.3. Comparison of computational complexity

The system used in the experiment is Windows10, the CPU is a 2.90 GHz i5 processor, memory is 16.0 GB, and the experimental software is the matlab2019a version. In the experiment, when the steady-state harmonic and transient harmonic are analyzed, each algorithm conducts 100 harmonic detection experiments respectively, and takes the average running time as the final result. The running time test results of the six harmonic detection methods are shown in Table 4.

Table 4. Comparison of computation complexity of detection methods

Method	WP	HMS	SST	HSST	EEWT	LMSST
Steady-state harmonic analysis	0.2746	0.7748	0.3926	0.4342	0.3645	0.4133
Transient harmonic analysis	0.2101	0.7059	0.3118	0.3844	0.2881	0.3398

It can be seen from Table 4 that the wavelet packet (WP) detection algorithm has the shortest calculation time, while the HMS algorithm has the longest calculation time because it needs to decompose the signal in an iterative way. The running time of the SST algorithm is basically the same as that of the EEWT algorithm. HSST and LMSST proposed in this paper need to further process the decomposition results of SST, so the running time of both HSST and LMSST is more than the SST algorithm. Compared with the EEWT method, the running time of the

LMSST method proposed in this paper is slightly longer, but the difference is not significant. It can be seen that the LMSST method can meet certain requirements in real-time and has good extensibility.

5. Conclusions

The LMSST algorithm is applied to power harmonic detection, and the harmonic/inter-harmonic detection method combining the local frequency maximum synchronous compression transform and synchronous extraction operator is proposed. The main conclusions are drawn from the detection results as follows:

1. LMSST can adaptively divide the signal spectrum according to the spectral extreme value of the signal, and accurately extract each harmonic or inter-harmonic component from the power system signal. This can effectively avoid the problem of modal mixing in traditional time-frequency analysis methods, and improve the extraction accuracy of harmonic/inter-harmonic components.
2. The WP method, HMS method, SST method, HSST method, EEWT method and LMSST method are used to detect the parameters of harmonics/inter-harmonics signals. Then the instantaneous amplitude and frequency of harmonics/inter-harmonics are calculated, and the starting and ending time of transient harmonics is located according to the instantaneous frequency.
3. The proposed method is suitable for the detection of steady-state and transient harmonics with high accuracy, and has good noise robustness when decomposing noisy signals. Furthermore, the proposed method also can be applied to the detection of harmonic/inter-harmonic parameters in a noisy background.

References

[1] Hou C., Zhu M., Chen Y., Cai X., *Pre-filter phase-locked loop: principles and effects with inter-harmonic perturbation*, IET Renewable Power Generation, vol. 14, no. 16, pp. 3088–3096 (2020), DOI: 10.1049/iet-rpg.2020.0448.

[2] Jove E., Gonzalev C.J.M., Casteleiro R.J.L. *et al.*, *An intelligent system for harmonic distortions detection in wind generator power electronic devices*, Neurocomputing, vol. 456, pp. 609–621 (2021), DOI: 10.1016/j.neucom.2020.07.155.

[3] Altintasi C., Aydin O., Taplamacioglu M.C. *et al.*, *Power system harmonic and interharmonic estimation using Vortex Search Algorithm*, Electric Power Systems Research, vol. 182, pp. 106187 (2020), DOI: 10.1016/j.epsr.2019.106187.

[4] Sun Y., Lin Y., Wang Y. *et al.*, *Theory of symmetric winding distributions and a general method for winding MMF harmonic analysis*, IET Electric Power Applications, vol. 14, no. 13 (2021), DOI: 10.1049/iet-epa.2020.0553.

[5] Cao Q., Shen Q.T., *An improved $i_p - i_q$ harmonic current detecting method and digital LPF filter's study*, Techniques of Automation and Applications, vol. 29, no. 3, pp. 74–76 (2010), http://en.cnki.com.cn/Article_en/CJFDTotal-ZDHJ201003022.htm.

[6] Paplinski J.P., Cariow A., *Fast 10-Point DFT Algorithm for Power System Harmonic Analysis*, Applied Sciences, vol. 11, no. 15, p. 7007 (2021), DOI: 10.3390/app11157007.

[7] Wu J.Z., Mei F., Chen C., *Power system harmonic detection method based on empirical wavelet transform*, Power System Protection and Control, vol. 48, no. 6, pp. 136–143 (2020), DOI: 10.19783/j.cnki.pspc.190470.

[8] Li J., Lin H., Teng Z. *et al*., *Digital prolate spheroidal window-based S-transform for time-varying harmonic analysis*, Electric Power Systems Research, vol. 187 (2020), DOI: 10.1016/j.epsr.2020.106512.

[9] Zhang Y.L., Chen H.W., *Parameter identification of harmonics and inter-harmonics based on ceemd-wpt and Prony algorithm*, Power System Protection and Control, vol. 46, no. 12, pp. 115–121 (2018), DOI: 10.7667/PSPC170866.

[10] Yang Y.K., Yang M.Y., *Application of prony algorithm in parameter identification of harmonics and inter-harmonics*, Proceedings of the CSU-EPSA, vol. 24, no. 3, pp. 121–126 (2012), http://en.cnki.com.cn/Article_en/CJFDTOTAL-DLZD201203024.htm.

[11] Zhang Y., Fan W., Zhang Q., Li X., *Harmonic separation from grid voltage with EEMD-ICA and SVD*, Computer Measurement and Control, vol. 27, no. 3, pp. 39–43 (2019), http://www.jsjclykz.com/ch/reader/view_abstract.aspx?file_no=201809061095.

[12] Chen Q., Cai W., Sun L. *et al*., *Harmonic detection method based on VMD*, Electrical Measurement and Instrumentation, vol. 55, no. 2, pp. 59–65 (2018), https://doi.org/10.1088/1742-6596/2095/1/012057.

[13] Thirumala K., Umarikar A.C., Jian T., *Estimation of single-phase and three -phase power -quality indices using empirical wavelet transform*, IEEE Transactions on Power Delivery, vol. 30, no. 1, pp.445–454 (2015), DOI: 10.1109/TPWRD.2014.2355296.

[14] Desai V.A., Rathore S., *Harmonic detection using Kalman filter*, In Proceedings of the 2016 International Conference on Electrical, Electronics, and Optimization Techniques (ICEEOT), Chennai, India, pp. 858–863 (2016), DOI: 10.1109/ICEEOT.2016.7754808.

[15] Tiyarachakun S., Areerak K.L., Areerak K.N., *Instantaneous Power Theory with Fourier and Optimal Predictive Controller Design for Shunt Active Power Filter*, Model. Simul. Eng., pp. 1–20 (2014), DOI: 10.1155/2014/381760.

[16] Habrouk M., Darwish M.K., *Design and implementation of a modified Fourier analysis harmonic current computation technique for power active filters using DSPs*, IEEE Proc. Electr. Power Appl., vol. 148, pp. 21–28 (2001), DOI: 10.1049/ip-epa:20010014.

[17] Karimi H., Karimi G.M., Reza I.M., Bakhshai A.R., *An adaptive filter for synchronous extraction of harmonics and distortions*, IEEE Trans. Power Deliv., vol. 18, pp. 1350–1356 (2003), DOI: 10.1515/ijeeps-2013-0145.

[18] Musa S., Mohd M.A., Hoon Y., *Modified Synchronous Reference Frame Based Shunt Active Power Filter with Fuzzy Logic Control Pulse Width Modulation Inverter*, Energies, vol. 10, no. 758 (2017), DOI: 10.3390/en10060758.

[19] Narongrit T., Areerak K.L., Areerak K.N., *A New Design Approach of Fuzzy Controller for Shunt Active Power Filter*, Electr. Power Compon. Syst., vol. 43, pp. 685–694 (2015), DOI: 10.1080/15325008.2014.996680.

[20] Sujitjorn S., Areerak K.L., Kulworawanichpong T., *The DQ Axis with Fourier (DQF) Method for Harmonic Identification*, IEEE Trans. Power Deliv., vol. 22, pp. 737–739 (2007), DOI: 10.1109/TPWRD.2006.882465.

[21] Daubechies I., Jianfeng L., *Synchrosqueezed wavelet transforms: An empirical mode decomposition-like tool*, Applied and Computational Harmonic Analysis, vol. 30, no. 2, pp. 243–261 (2011), DOI: 10.1016/j.acha.2010.08.002.

[22] Li L., Cai H.Y., Jiang Q.T., Ji H.B., *Adaptive synchrosqueezing transformwith a time-varying parameter for non-stationary signal separation*, Applied and Computational Harmonic Analysis, vol. 49, no. 3, pp. 1884–2020 (2019), DOI: 10.1016/j.acha.2019.06.002.

[23] Gang Y., Zhonghu W., Ping Z., Zhen L., *Local maximum synchrosqueezing transform: An energy-concentrated time-frequency analysis tool*, Mechanical Systems and Signal Processing, vol. 117, pp. 537–552 (2019), DOI: 10.1016/j.ymssp.2018.08.006.

[24] Lin L., Haiyan C., Qiangtang J., Hongbing J., *An empirical signal separation algorithm for multicomponent signals based on linear time-frequency analysis*, Mechanical Systems and Signal Processing. vol. 121, pp. 791–809 (2019), DOI: 10.1016/j.ymssp.2018.11.037.

[25] Rasoul M.M., Alan F.L., Yunwei L., *Adaptive control of an active power filter for harmonic suppression and power factor correction*, International Journal of Dynamics and Control, pp. 1–10 (2021), DOI: 10.1007/s40435-021-00825-0.

[26] Avalos O., Cuevas E., Becerra H.G. *et al.*, *Kernel Recursive Least Square Approach for Power System Harmonic Estimation*, Electric Power Components and Systems, vol. 48, no. 16–17, pp. 1708–1721 (2021), DOI: 10.1080/15325008.2021.1908457.

[27] Mert A., Celik H.H., *Emotion recognition using time-frequency ridges of EEG signals based on multivariate synchrosqueezing transform*, Biomedizinische Technik. Biomedical Engineering, vol. 66, no. 4, pp. 345–352 (2021), DOI: 10.1515/bmt-2020-0295.

[28] Yang C., Ban L., *Research on Harmonic Detection System Based on Wavelet Packet Transform*, IOP Conf. Series: Journal of Physics: Conf. Series, vol. 1314, no. 012038 (2019), DOI: 10.1088/1742-6596/1314/1/012038.

[29] Gong M.F. *et al.*, *A New Method to Detect Harmonics and Inter-Harmonics Based on Hilbert Marginal Spectrum*, Applied Mechanics and Materials, vol. 229–231, pp. 1060–1063 (2012), DOI: 10.4028/www.scientific.net/AMM.229-231.1060.

[30] Yu M., Wang B., Wang W.B. *et al.*, *An inter-harmonic detection method based on synchrosqueezing wavelet transform*, Proceedings of the CSEE, vol. 36, no. 11, pp. 2944–2951 (2016), DOI: 10.13334/j.0258-8013.pcsee.2016.11.010.

[31] Chang G.W. *et al.*, *A Hybrid Approach for Time-Varying Harmonic and Interharmonic Detection Using Synchrosqueezing Wavelet Transform*, Applied Sciences, vol. 11, no. 2, pp. 752 (2021), DOI: 10.3390/app11020752.

[32] Khoa N.M., Le V.D., Tung D.D., Toan N.A., *An advanced IoT system for monitoring and analysing chosen power quality parameters in micro-grid solution*, Archives of Electrical Engineering, vol. 70, no. 1, pp. 173–188 (2021), DOI: 10.24425/aee.2021.136060.

[33] Yudaev I.V., Rud E.V., Yundin M.A., Ponomarenko T.Z., Isupova A.M., *Analysis of the harmonic composition of current in the zero-working wire at the input of the load node with the prevailing non-linear power consumers*, Archives of Electrical Engineering, vol. 70, no. 2, pp. 463–473 (2021), DOI: 10.24425/aee.2021.136996.